

Conditional Mass Functions and Merger Rates of Dark Matter Halos in the Ellipsoidal Collapse Model

Jun Zhang^{1*}, Chung-Pei Ma¹, Onsi Fakhouri¹

¹ 601 Campbell Hall, Department of Astronomy, University of California, Berkeley, CA 94720, USA

3 March 2019

ABSTRACT

Analytic models based on spherical and ellipsoidal gravitational collapse have been used to derive the mass functions of dark matter halos and their progenitors (the *conditional* mass function). The ellipsoidal model generally provides a better match to simulation results, but there has been no simple analytic expression in this model for the conditional mass function that is accurate for small time steps, a limit that is important for generating halo merger trees and computing halo merger rates. We remedy the situation by deriving accurate analytic formulae for the first-crossing distribution, the conditional mass function, and the halo merger rate in the ellipsoidal collapse model in the limit of small look-back times. We show that our formulae provide a closer match to the Millennium simulation results than those in the spherical collapse model and the ellipsoidal model of Sheth & Tormen (2002).

Key words:

galaxies: clusters: general - cosmology: theory - dark matter

1 INTRODUCTION

Press & Schechter (1974) presented an analytical expression for the unconditional mass function of dark matter halos at redshift z , $n(M, z)$, based on the spherical collapse model. This function is closely related to the first-crossing distribution of random walks with a barrier in the excursion set framework (Bond et al. 1991). In this framework, the linear over-density computed at a given point in the Lagrangian space fluctuates as a Markovian process when smoothed on successively smaller scales, and a dark matter halo is identified at the point when the random walk of the linear over-density crosses a critical value, or a barrier $\mathcal{B}(M, z)$. In the spherical collapse model, this barrier depends only on time and is independent of mass: $\mathcal{B} = \delta_c/D(z)$, where $\delta_c = 1.68$ and $D(z)$ is the standard linear growth factor.

Although analytically simple, the spherical collapse model has been found to over-predict the abundance of small halos and under-predict that of massive ones (*e.g.*, Lacey & Cole 1994; Gelb & Bertschinger 1994; Tormen 1998; Sheth & Tormen 1999). The reason is mainly that halo collapses are generally triaxial rather than spherical (*e.g.*, Doroshkevich 1970; Bardeen et al. 1986). Based on Bond & Myers (1996), Sheth et al. (2001) use the ellipsoidal collapse model and obtain fitting functions that provide a

closer match to the halo mass function in N-body simulations. Unlike the spherical collapse model in which the condition for the virialization of a dark matter halo is solely determined by the linear over-density on the scale of the halo mass; the virialization condition in the ellipsoidal collapse model also depends on halo ellipticity and prolateness. By assuming that a dark matter halo becomes virialized when its third axis collapses, Sheth et al. (2001) find a new criterion for the virialization of dark matter halos, which involves all three parameters. They further simplify the virialization condition by fixing the ellipticity and the prolateness at their most likely values for a given over-density, and obtain a fitting formula for the barrier $\mathcal{B}(M, z)$ that is mass-dependent, in contrast to the constant $\mathcal{B}(z)$ of the spherical collapse model. A mass-dependent barrier is commonly referred to as a *moving* barrier, and it is this mass-dependence that suppresses the abundance of small halos while increasing that of massive ones in the ellipsoidal collapse model. Physically, this is because a smaller halo typically has a larger ellipticity and therefore a longer collapsing time.

The relationship between the unconditional mass function and the first crossing distribution associated with barrier-crossing random walks has been extended to obtain the *conditional* mass function of halos (Bond et al. 1991; Lacey & Cole 1993). In this so-called extended Press-Schechter (EPS) model, the conditional mass function $dN(M_1, z_1|M_0, z_0)/dM_1$ gives the average number of pro-

* E-mail: jzhang@astro.berkeley.edu

genitor halos (of mass M_1 at redshift z_1) per unit mass associated with a descendant halo of mass M_0 at redshift z_0 ($z_1 > z_0$). Once determined, it can be used to generate merger trees of halos for many applications (e.g., galaxy formation, growth of the central black hole, reionization) using Monte Carlo simulations.

The conditional mass function has a simple analytic form in the constant barrier spherical collapse model (Lacey & Cole 1993). For a moving barrier (such as the ellipsoidal collapse model), however, exact analytic forms have been found only for the special case of a linear barrier (Sheth & Tormen 2002); while the same authors have proposed an approximate form for a general moving barrier. We find that none of these formulae work well for $z_1 - z_0 \ll 1$, which are required for generating accurate merger trees in most Monte Carlo methods (e.g., Lacey & Cole 1993; Kauffmann & White 1993; Somerville & Kolatt 1999; Cole et al. 2000) and for relating halo merger rates to the conditional mass function (§ 2 below). Fakhouri & Ma (2007) directly compare the halo merger rates determined from the Millennium simulation (Springel et al. 2005) and the prediction of the spherical collapse EPS model, finding the latter to overpredict the major merger rates by up to a factor of ~ 2 and underpredict the minor merger rates by up to a factor of ~ 5 . Recently various other fitting forms for the conditional mass function have been proposed that are calibrated to the results from particular N -body simulations, e.g., Cole et al. (2007); Parkinson et al. (2007); Neistein & Dekel (2007). An alternative way of deriving the conditional mass function that does not rely explicitly on fitting to simulations is to solve the integral equation proposed by Zhang & Hui (2006). This method, which is based on the conservation of probability in the excursion set formalism, is accurate but computationally expensive.

In §2, we derive almost exact analytic forms for the first crossing distribution, the conditional mass function, and the halo merger rate in the ellipsoidal collapse model in the limit of small look-back times; a limit where earlier work breaks down. Our method is based on Zhang & Hui (2006), but our results are expressed in simple analytic forms. We compare the predictions of this improved ellipsoidal collapse model with those from the spherical collapse model and the Millennium simulation in §3.

This paper assumes the cosmological parameters used in the Millennium simulation (Springel et al. 2005) : $\Omega_m = 0.25$, $\Omega_b = 0.045$, $h = 0.73$, $\Omega_\Lambda = 0.75$, $n = 1$, $\sigma_8 = 0.9$,

2 IMPROVED ELLIPSOIDAL COLLAPSE MODEL FOR SMALL TIME STEPS

We use $dN(M_1, z_1|M_0, z_0)/dM_1$ to denote the conditional mass function of dark matter halos, defined in §1. We use $B_M(M_1, M_2, z)dM_1dM_2$ to denote the merger rate of halos, which is defined to be the number of mergers between halos of mass (M_1, M_1+dM_1) and (M_2, M_2+dM_2) per unit volume and unit redshift at redshift z . If halo mergers are assumed to be binary and mass conserving such that the consequence of each merger is the formation of a descendent halo of mass $M_0 = M_1 + M_2$, then we can related the merger rate to the (number-weighted) conditional mass function through a simple relation (see Fakhouri & Ma 2007 for a detailed

discussion):

$$\begin{aligned} & B_M(M_1, M_2, z)dM_1dM_2 \\ &= n(M_1 + M_2, z)d(M_1 + M_2) \\ &\times \frac{1}{\Delta z} \frac{d}{dM_1} N(M_1, z + \Delta z|M_1 + M_2, z)dM_1 \end{aligned} \quad (1)$$

where $n(M, z)$ is the (unconditional) halo mass function at redshift z , and Δz is assumed to be small.

To study how many progenitors at redshift z_1 are associated with a descendant halo of mass M_0 at z_0 , we let the random walk of the linear over-density start from the scale of the descendant halo $S(M_0)$ with an over-density of $\mathcal{B}[S(M_0), z_0]$, where $S(M) = \sigma^2(M)$ is the variance of the linear density field smoothed with a window function containing mass M . A progenitor of mass M_1 is then identified once the random walk crosses $\mathcal{B}[S(M_1), z_1]$ on the scale of $S(M_1)$. Consequently, the conditional mass function can be written as:

$$M_1 \frac{d}{dM_1} N(M_1, z_1|M_0, z_0)dM_1 = M_0 f(\Delta S) d\Delta S \quad (2)$$

where $\Delta S = S(M_1) - S(M_0)$, and $f(\Delta S)$ is the first-crossing distribution of random walks with a barrier of the form $b(\Delta S) = \mathcal{B}[S(M_1), z_1] - \mathcal{B}[S(M_0), z_0]$.

As mentioned in § 1, analytic solutions for $f(\Delta S)$ have only been found when the barrier is a constant or a linear function of ΔS . Here we propose an almost exact analytic solution for the first-crossing distribution in the limit of $z_1 - z_0 \ll 1$. We use the fact that the barrier $b(\Delta S)$ is a weakly nonlinear function of ΔS (Zhang & Hui 2006) to approximate it by

$$b(\Delta S) = b_0 + b_1 \Delta S + b_2 (\Delta S)^2, \quad (3)$$

where $b_2 (\Delta S)^2$ is assumed to be subdominant in comparison with the other two terms¹. The first-crossing distribution can then be written as $f(\Delta S, b_0, b_1, b_2)$. When $b_2 = 0$, $f(\Delta S, b_0, b_1, 0)$ has the analytic form (Sheth & Tormen 2002):

$$f(\Delta S, b_0, b_1, 0) = \frac{b_0}{\Delta S \sqrt{2\pi \Delta S}} \exp \left[-\frac{(b_0 + b_1 \Delta S)^2}{2\Delta S} \right] \quad (4)$$

For nonzero b_2 , we approximate $f(\Delta S, b_0, b_1, b_2)$ as

$$\begin{aligned} f(\Delta S, b_0, b_1, b_2) &\approx f(\Delta S, b_0, b_1, 0) \\ &+ b_2 \times \partial_{b_2} f(\Delta S, b_0, b_1, b_2)|_{b_2=0} \end{aligned} \quad (5)$$

and derive the second term on the right side of eq. (5) next.

For simplicity, we denote ΔS as s and $f(s, b_0, b_1, b_2)$ as $f(s)$. The first-crossing distribution $f(s)$ in general satisfies the integral equation (Zhang & Hui 2006):

$$f(s) = g_1(s) + \int_0^s ds' f(s') g_2(s, s') \quad (6)$$

where

$$g_1(s) = \left[\frac{b(s)}{s} - 2 \frac{db}{ds} \right] P_0 [b(s), s] \quad (7)$$

¹ This is obviously not true when ΔS is very large. But we find that in practice, the relevant range of ΔS is rarely large enough to invalidate the assumption.

$$g_2(s, s') = \left[2 \frac{db}{ds} - \frac{b(s) - b(s')}{s - s'} \right] P_0 [b(s) - b(s'), s - s']$$

$$P_0(\delta, s) = \frac{1}{\sqrt{2\pi}s} \exp\left(-\frac{\delta^2}{2s}\right)$$

From eq. (6) and after some algebra, we find

$$\partial_{b_2} f(s)|_{b_2=0} = g(s) + \int_0^s ds' \partial_{b_2} f(s') g_2(s, s')|_{b_2=0}, \quad (8)$$

where

$$g(s) = -b_0^2 \times P_0(b_0 + b_1 s, s) \quad (9)$$

$$+ \int_0^s ds' f(s', b_0, b_1, 0) (b_1^2 s'^2 - s') P_0 [b_1(s - s'), s - s']$$

$$g_2(s, s')|_{b_2=0} = b_1 \times P_0 [b_1(s - s'), s - s']. \quad (10)$$

The two terms in $g(s)$ come from $\partial_{b_2} g_1$ and $\partial_{b_2} g_2$ respectively, and a number of terms have been cancelled out using the relation $\int_0^s ds' f(s', b_0, b_1, 0) P_0 [b_1(s - s'), s - s'] = P_0((b_0 + b_1 s, s))$ that follows from eq. (6) for $b_2 = 0$.

The complicated form of $g(s)$ in eq. (9) makes it difficult to solve eq. (8). However, we are interested in the limit of small look-back times for the conditional mass function, which corresponds to a small barrier difference $b(s)$. We can thus neglect the terms of $\mathcal{O}(b_0^2)$ and simplify g as²:

$$g(s) \approx \frac{b_0}{4} (b_1^2 s - 2) \exp\left(-\frac{b_1^2 s}{2}\right). \quad (11)$$

We then solve for $\partial_{b_2} f(s)$ by combining eqs. (8), (10), and (11) and using the Laplace transform:

$$\partial_{b_2} f(s)|_{b_2=0} = -\frac{b_0}{4} \exp\left(-\frac{b_1^2 s}{2}\right) \left[1 + \frac{b_1 \sqrt{s}}{\Gamma(3/2)} \right]. \quad (12)$$

Substituting this expression back into eq. (5), we obtain the first-crossing distribution for a barrier of the form $b(\Delta S) = b_0 + b_1 \Delta S + b_2 (\Delta S)^2$:

$$f(\Delta S) = \frac{b_0}{\Delta S \sqrt{2\pi \Delta S}} \exp\left[-\frac{(b_0 + b_1 \Delta S)^2}{2\Delta S}\right] \quad (13)$$

$$- \frac{b_0 b_2}{4} \exp\left(-\frac{b_1^2 \Delta S}{2}\right) \left[1 + \frac{b_1 \sqrt{\Delta S}}{\Gamma(3/2)} \right] + \mathcal{O}(b_0^2).$$

This is our main result. We note that this equation reduces to the analytic expressions of eq. (4) in the spherical collapse model (i.e. a constant barrier with $b_1 = b_2 = 0$) and the ellipsoidal model with a linear barrier (i.e. $b_2 = 0$). The second term on the right hand side of eq. (13) is a new term arising from the quadratic part of $b(\Delta S)$. This term is absent in the analytic approximation proposed in eq. (7) of Sheth & Tormen (2002). The latter is obtained by replacing the barrier \mathcal{B} and the variance S in their unconditional mass function in the ellipsoidal model with

² Note that eq.(11) is derived by neglecting the first term on the right side of eq.(9) and approximating $f(s', b_0, b_1, 0)$ (eq.(4)) as $b_0/\sqrt{2\pi s^3} \times \exp(-b_1^2 s/2)$. These approximations introduce errors of order b_0^2 to $g(s \gg b_0^2)$ and of order b_0 to $g(s \sim b_0^2)$. Similarly, the error on $\partial_{b_2} f(s)$ is of order b_0^2 when $s \gg b_0^2$, and of order b_0 when $s \sim b_0^2$. We find that this error is negligible when b_0 is small.

$\mathcal{B}(S(M_1), z_1) - \mathcal{B}(S(M_0), z_0)$ and $S(M_1) - S(M_0)$, respectively; that is, they assume that the unconditional and conditional mass functions have the same form. This assumption holds exactly in the spherical case but is not so for ellipsoidal collapse. As we illustrate in Fig. 1 below, their expression for the conditional mass function becomes inaccurate for small look-back times.

We can now use eq. (2) to convert our first-crossing distribution in eq. (13) into the conditional mass function. To compute the barrier difference $b(\Delta S) = \mathcal{B}[S(M_1), z_1] - \mathcal{B}[S(M_0), z_0]$, we use the barrier shape from Sheth et al. (2001) and Sheth & Tormen (2002) that has been shown to provide close fits for the *unconditional* mass function:

$$\mathcal{B}[S(M), z] = \sqrt{\gamma} \omega(z) [1 + \beta(\gamma \nu)^{-\alpha}] \quad (14)$$

where $\alpha = 0.615$, $\beta = 0.485$, $\gamma = 0.75$, $\nu = \omega^2(z)/S(M)$, $\omega(z) = \delta_c/D(z)$, $\delta_c = 1.68$, and $D(z)$ is the linear growth factor. The resulting conditional mass function in our ellipsoidal collapse model for $z_1 - z_0 \ll 1$ is:

$$\frac{d}{dM_1} N(M_1, z_1 | M_0, z_0) = \frac{d}{dM_1} N(M_1, z_1 | M_0, z_0) \Big|_{\text{sph}} \quad (15)$$

$$\times A_0 \exp\left(-\frac{A_1^2 \Delta S}{2}\right) \left\{ 1 + A_2 \left[\frac{\Delta S}{S(M_0)} \right]^{\frac{3}{2}} \left[1 + \frac{A_1 \sqrt{\Delta S}}{\Gamma(3/2)} \right] \right\}$$

where $dN/dM_1|_{\text{sph}} = (M_0/M_1)(dS_1/dM_1)(\Delta\omega/\Delta S \sqrt{2\pi \Delta S})$ is the standard spherical model result, $A_0 = 0.866(1 - 0.133\nu_0^{-0.615})$, $A_1 = 0.308\nu_0^{-0.115} S(M_0)^{-0.5}$, $A_2 = 0.0373\nu_0^{-0.115}$, $\nu_0 = \omega^2(z_0)/S(M_0)$, and $\Delta\omega = \omega(z_1) - \omega(z_0)$. The values of A_0 , A_1 , and A_2 are closely related to the parameters b_0, b_1 , and b_2 in the barrier in eqs.(3) and (13). We note that in eq. (15), barrier crossing leads to a negative A_0 when $S(M_0) \gtrsim 30 S^*(z_0)$, where $S^* = \omega^2(z_0)$. Since this problem only arises when the descendant mass is much smaller than the typical halo mass at redshift z_0 , it should occur very rarely.

We can now use eqs. (1) and (15) to write down an analytic expression for the halo merger rate. Following the notation of Fakhouri & Ma (2007), we express the merger rate in terms of the total descendent mass $M_0 = M_1 + M_2$ and the mass ratio of the two progenitors $\xi = M_2/M_1$ (assuming $\xi \leq 1$ without loss of generality), and use $B(M_0, \xi, z) dM_0 d\xi = B_M(M_1, M_2, z) dM_1 dM_2$ to relate the two rates. We find

$$\frac{B(M_0, \xi, z)}{n(M_0, z)} = \frac{B(M_0, \xi, z)}{n(M_0, z)} \Big|_{\text{sph}} \quad (16)$$

$$\times A_0 \exp\left(-\frac{A_1^2 \Delta S_i}{2}\right) \left\{ 1 + A_2 \left[\frac{\Delta S_i}{S(M_0)} \right]^{\frac{3}{2}} \left[1 + \frac{A_1 \sqrt{\Delta S_i}}{\Gamma(3/2)} \right] \right\}$$

where $\Delta S_i = S(M_i) - S(M_0)$, and the prediction from the spherical collapse model is

$$\frac{B(M_0, \xi, z)}{n(M_0, z)} \Big|_{\text{sph}} = \frac{d\omega}{dz} \frac{M_0^2}{(1 + \xi)^2 M_i} \frac{dS(M_i)}{dM_i} \frac{1}{\Delta S_i \sqrt{2\pi \Delta S_i}} \quad (17)$$

where M_i can be either of the progenitors M_1 or M_2 . We recall that the conditional mass function and the merger rate in the EPS model is not symmetric with respect to the two progenitor masses. This remains an unsolved problem, which we will discuss in more detail in a companion paper (Zhang et al. 2008). Below we simply show the results for

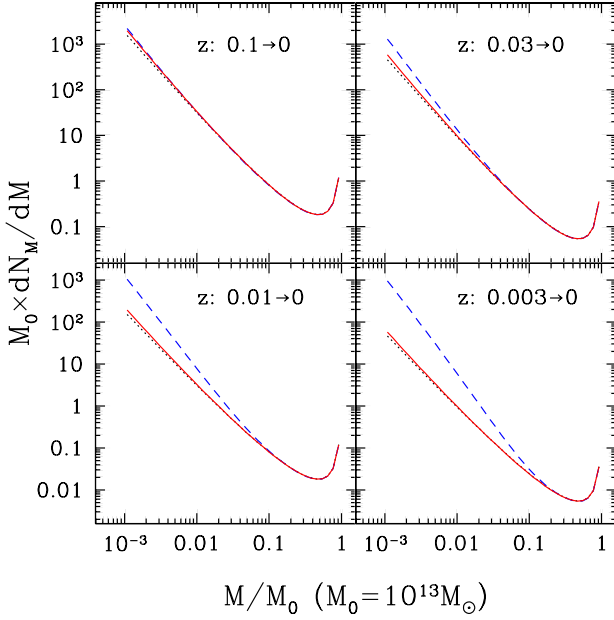


Figure 1. The conditional mass functions for the progenitor halos of a descendant halo of mass $M_0 = 10^{13} M_\odot$ at redshift zero. The four panels are for four look-back times: $\Delta z = 0.1, 0.03, 0.01$, and 0.003 . Eq. (15) of this paper (red solid curves) agrees closely with the exact solution from the method of Zhang & Hui (2006) (black dotted), while the approximation based on eq. (7) of Sheth & Tormen (2002) (blue dashed) overpredicts the number of progenitors for small look-back time ($\Delta z \lesssim 0.03$).

both choices. According to the notation of Fakhouri & Ma (2007), we call the merger rate “option A” when M_i is assigned to the smaller progenitor M_2 , and “option B” when $M_i = M_1$.

3 NUMERICAL RESULTS AND COMPARISON WITH THE MILLENNIUM SIMULATION

In Fig. 1, we illustrate the accuracy of eq. (15) by comparing it with the exact solution from Zhang & Hui (2006) and the analytic approximation based on eq. (7) of Sheth & Tormen (2002). The figure shows the conditional mass functions of four different look-back times ($\Delta z = 0.1, 0.03, 0.01, 0.003$) for a descendant halo of mass $10^{13} M_\odot$ at redshift zero. The approximation of Sheth & Tormen (2002) is seen to overpredict the number of lower mass progenitors by up to a factor of 2 to 10 for $\Delta z \lesssim 0.03$, whereas eq. (15) of this paper is accurate when Δz is as small as 0.003.

For the halo merger rate, we compare the predictions of our ellipsoidal model with the Millennium simulation merger rate determined by Fakhouri & Ma (2007) using the “stitching” method. They found that the halo merger rate in the simulation converges well when the look-back time Δz approaches zero and can be described by a simple universal fitting formula:

$$\frac{B(M_0, \xi, z)}{n(M_0, z)} = A \left(\frac{M_0}{\tilde{M}} \right)^{\alpha_1} \xi^{\alpha_2} \exp \left[\left(\frac{\xi}{\tilde{\xi}} \right)^{\alpha_3} \right] \left[\frac{d\omega(z)}{dz} \right]^{\alpha_4} \quad (18)$$

where $\tilde{M} = 1.2 \times 10^{12} M_\odot$, $\tilde{\xi} = 0.098$, $A = 0.0289$, $\alpha_1 = 0.083$, $\alpha_2 = -2.01$, $\alpha_3 = 0.409$, and $\alpha_4 = 0.371$. Their Fig. 15 illustrates the large discrepancy between equation (18) and the prediction of the standard spherical EPS model.

Figs. 2 (for option A) and 3 (option B) show the ratio between the halo merger rate B/n of our ellipsoidal collapse model (eq. (16)) and that of the Millennium simulation (eq. (18)). The spherical collapse model (eq. (17)) is also shown for comparison. The plots are made for three descendant halo masses ($M_0 = 10^{12}, 10^{13}, 10^{14} M_\odot$) and four redshifts ($z = 0, 1, 2, 3$). The minimum halo mass is chosen to be $2 \times 10^{10} M_\odot$ as set by the halo mass resolution in the Millennium simulation. Comparison of the two figures shows that the two choices of M_i give similar results for major mergers but yield very different predictions for $\xi \ll 1$, where option A (Fig. 2) agrees better with the Millennium than option B (Fig. 3). We note that the two options predict different power-law dependencies on ξ at $\xi \ll 1$: for $S(M) \propto M^{-\gamma}$, option A gives $B/n \propto \xi^{\gamma/2-2}$, but option B gives $B/n \propto \xi^{-1.5}$, which is independent of the density variance on the scale of the smaller progenitor mass. It is also interesting to note that option A is implicitly used in some Monte Carlo methods; for example, Cole et al. (2000) select the mass of the first progenitor from the lower half of the conditional mass function (i.e. $M_i < M_0/2$).

According to Fig. 2, the discrepancy between our ellipsoidal collapse model and the Millennium simulation is typically 20 ~ 30%, but can reach up to about 80% when $\xi \sim 1$. On the other hand, the relative difference between the spherical collapse model and Millennium is typically 40% ~ 60%, and reaches up to 120% for the major mergers. Therefore in almost every case, the new ellipsoidal collapse model improves the agreement with the Millennium simulation.

4 SUMMARY

We have derived new analytic formulae for the first-crossing distribution (eq. (13)), the conditional mass function (eq. (15)), and the merger rate of dark matter halos (eq. (16)) in the ellipsoidal collapse model in the limit of small look-back times. Our method is based on solving the first-crossing distribution of random walks with a moving barrier using the exact integral equation of Zhang & Hui (2006). This method results in extra terms in eqs. (13), (15), and (16) that are absent in the spherical collapse model and the ellipsoidal model of Sheth & Tormen (2002). Fig. 1 illustrates how these terms correct the discrepancies of Sheth & Tormen (2002) in the conditional mass function for small look-back times $\Delta z \lesssim 0.03$.

Eq. (1) relates the conditional mass function at small Δz to the halo merger rate. The halo merger rate of our ellipsoidal collapse model generally agrees better with the Millennium result reported in Fakhouri & Ma (2007) than that of the spherical collapse model (red vs blue curves in Figs. 2 and 3). The discrepancy between our ellipsoidal collapse model and the Millennium simulation is typically 20% ~ 30%, which is about a factor of two smaller than that of the spherical collapse model. A comparison between Figs. 2 and 3 shows a better agreement between model and

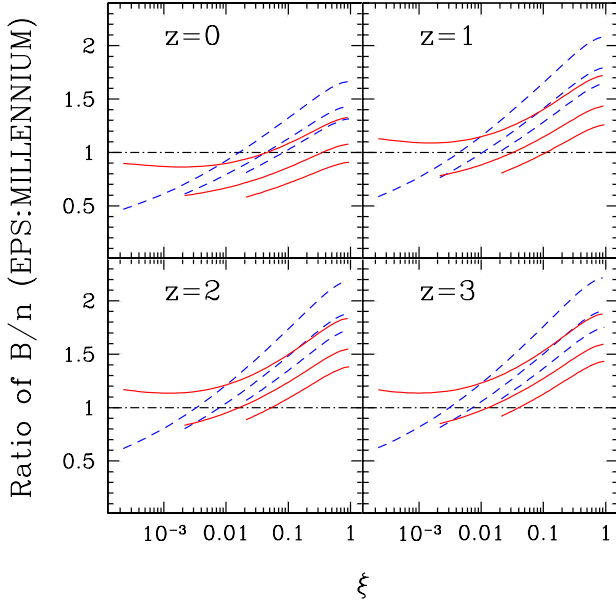


Figure 2. Comparison of the halo merger rates from our ellipsoidal model predictions (eq.(16,17)) vs. the Millennium simulation (eq.(18)). The different panels show the merger rates at four redshifts: $z = 0, 1, 2, 3$. Within each panel, the red solid curves show the ratio of our ellipsoidal collapse model prediction (eq.(16)) to the Millennium result; the blue dashed curves show the ratio of the standard spherical collapse model (eq.(17)) to the Millennium. For each color, the set of three curves show three descendant halo masses (from bottom up): 10^{12} , 10^{13} , and $10^{14} M_{\odot}$. The progenitor mass M_i in eqs. (17) and (16) is chosen to be the less massive M_2 (option A), which is our preferred option.

simulation when the progenitor mass M_i in the analytic formulae is assigned to be the smaller progenitor (option A).

A number of factors can contribute to the remaining 20% to 30% discrepancy between the model and the simulation. These include the statistical importance of non-binary mergers, diffuse accretion and tidal stripping of halo mass (such that $M_0 \neq M_1 + M_2$), and the impact of a halo's environment on merger rates that can lead to non-Markovian processes in the excursion set model (Neistein & Dekel 2007).

Our conditional mass function in eq.(15) can be easily incorporated into Monte Carlo simulations to study halo merger histories over a large look-back time. This is done in a companion paper (Zhang et al. 2008), in which we compare several existing Monte Carlo algorithms (*e.g.*, Lacey & Cole 1993; Kauffmann & White 1993; Somerville & Kolatt 1999; Cole et al. 2000) that are all based on the spherical collapse model, and propose a more accurate method using eq.(15). Several groups have recently proposed accurately parameterized forms of the conditional mass function based on fits to the Millennium results and incorporated them into different Monte Carlo simulations (Cole et al. 2007; Parkinson et al. 2007; Neistein & Dekel 2007). As we will show in Zhang et al. (2008), a similar level of accuracy can be achieved using eq.(15) of this paper and our Monte Carlo method without a priori knowledge of N-body simulations.

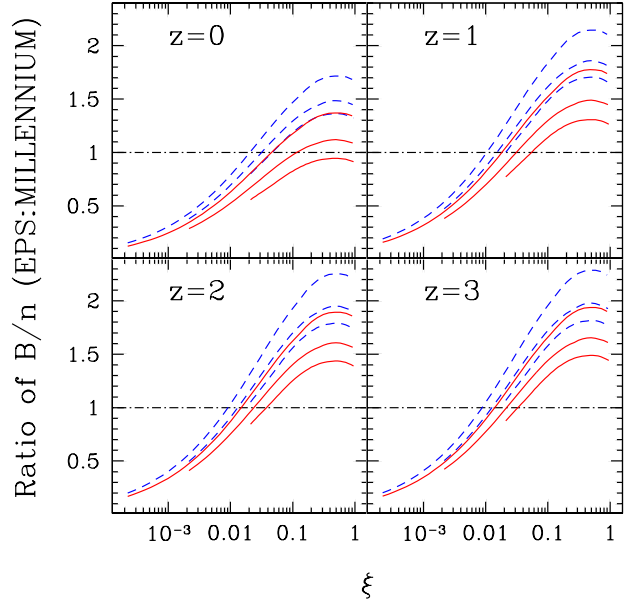


Figure 3. Same as Fig. 2, except that the progenitor mass M_i in both eq. (17) and (16) is chosen to be the more massive progenitor M_1 (option B), which is not our preferred option.

We thank James Bullock, Joanne Cohn, Lam Hui, Ravi Sheth, Martin White, Simon White for useful discussions. This work is supported in part by NSF grant AST 0407351. The Millennium Simulation databases used in this paper and the web application providing online access to them were constructed as part of the activities of the German Astrophysical Virtual Observatory.

REFERENCES

- Bardeen J., Bond J., Kaiser N., Szalay A., 1986, ApJ, 304, 15
- Bond J., Cole S., Efstathiou G., Kaiser N., 1991, ApJ, 379, 440B
- Bond J. & Myers S., 1996, ApJS, 103, 1
- Cole S., Helly J., Frenk, C. S., Parkinson, H. arXiv:0708.1376
- Cole S., Lacey C., Baugh C., Frenk C., 2000, MNRAS, 319, 168
- Doroshkevich A., 1970, Astrofizika, 3, 175
- Fakhouri O. & Ma C.-P., 2007, arXiv:0710.4567
- Gelb J. & Bertschinger, 1994, ApJ, 436, 467
- Kauffmann G. & White S., 1993, MNRAS, 261, 921
- Lacey C. & Cole S., 1993, MNRAS, 262, 627
- Lacey C. & Cole S., 1994, MNRAS, 271, 676
- Neistein E. & Dekel A., 2007, astro-ph/0708.1599
- Parkinson, H., Cole S., Helly, J. arXiv:0708.1382
- Press W. & Schechter P., 1974, ApJ, 187, 425
- Sheth R. & Tormen G., 1999, MNRAS, 308, 119
- Sheth R., Mo H., Tormen G., 2001, MNRAS, 323, 1
- Sheth R. & Tormen G., 2002, MNRAS, 329, 61 [ST02]
- Somerville R. & Kolatt T., 1999, MNRAS, 305, 1
- Springel V. et al., 2005, Nature, 435, 629

Tormen G., 1998, MNRAS, 297, 648

Zhang J. & Hui L., 2006, ApJ, 641, 641 [ZH06]

Zhang J., Ma C.-P., Fakhouri O., 2008, in preparation